The huntingtin N17 domain is a multifunctional CRM1 and Ran-dependent nuclear and cilial export signal

T. Maiuri, T. Woloshansky, J. Xia and R. Truant[*]

Department of Biochemistry and Biomedical Sciences, McMaster University, 1200 Main Street West, Hamilton, ON, Canada L8N3Z5

The first 17 amino acids of Huntington's disease (HD) protein, huntingtin, comprise an amphipathic alpha-helical domain that can target huntingtin to the endoplasmic reticulum (ER). N17 is phosphorylated at two serines, shown to be important for disease development in genetic mouse models, and shown to be modified by agents that reverse the disease phenotype in an HD mouse model. Here, we show that the hydrophobic face of N17 comprises a consensus CRM1/exportin-dependent nuclear export signal, and that this nuclear export activity can be affected by serine phospho-mimetic mutants. We define the precise residues that comprise this nuclear export sequence (NES) as well as the interaction of the NES, but not phospho-mimetic mutants, with the CRM1 nuclear export factor. We show that the nuclear localization of huntingtin depends upon the RanGTP/GDP gradient, and that N17 phosphorylation can also distinguish localization of endogenous huntingtin between the basal body and stalk of the primary cilium. We present a mechanism and multifunctional role for N17 in which phosphorylation of N17 not only releases huntingtin from the ER to allow nuclear entry, but also prevents nuclear export during a transient stress response event to increase the levels of nuclear huntingtin and to regulate huntingtin access to the primary cilium. Thus, N17 is a master localization signal of huntingtin that can mediate huntingtin localization between the cytoplasm, nucleus and primary cilium. This localization can be regulated by signaling, and is misregulated in HD.

INTRODUCTION

Huntington's disease (HD) is an autosomal-dominant, age-onset neurodegenerative disorder for which there is no treatment. HD is caused by a CAG DNA expansion in the first exon of the *IT15* gene, which translates to an expanded polyglutamine tract in the mutant huntingtin protein (1). The polyglutamine region is encoded immediately downstream of the first 17 amino acids of huntingtin, termed the N17 domain.

The N17 domain forms an amphipathic alpha helix (2–6), and is subject to multiple post-translational modifications including phosphorylation (3,7,8), acetylation (8) and sumoylation (9). In HD, mouse-derived striatal cells, polyglutamine-expanded huntingtin is hypo-phosphorylated at serines 13 and 16 within the N17 domain (3). The phosphorylation state of these residues is known to influence mutant huntingtin-mediated toxicity in a cell-based model (3), and HD phenotypes are abolished in BAC transgenic mice expressing phospho-mimetic (S13D/S16D) polyglutamine-expanded alleles, but not in those expressing the phospho-resistant S13A/S16A alleles (10). Furthermore, treatment of symptomatic HD mice with the ganglioside GM1, which restores N17 phosphorylation in mutant huntingtin, also restores normal motor function (11).

The phosphorylation state and alpha-helical structure of N17 participate in the regulation of huntingtin subcellular localization. N17 has been reported to mediate mitochondrial, endoplasmic reticulum (ER) and Golgi localization (5,12), as a translocated promoter region (TPR)-dependent nuclear export signal (13), as a 'cytoplasmic retention-like domain' (14) and as a membrane-binding domain mediating ER, late endosomal and autophagic vesicle localization (4). We have previously

[*]To whom correspondence should be addressed. Tel: +905-525-9140; Fax: +905-522-9033; Email: truantr@mcmaster.ca

shown that mutations and post-translational modifications resulting in the loss of N17 alpha-helical content result in nuclear accumulation of N17–YFP fusion proteins and of endogenous, full-length huntingtin (3,4). Furthermore, antibodies that distinguish between unphosphorylated and phosphorylated N17 states display distinct subcellular patterns. Unmodified N17 huntingtin shows diffuse cytoplasmic and ER localization, whereas phosphorylated N17 huntingtin is detected at centrosomes, the mitotic spindle and cytokinetic cleavage furrow, and at chromatin-dependent nuclear puncta (3). Huntingtin subcellular localization is also regulated by a nuclear export sequence (NES) recognized by the nuclear export factor Chromosome region maintenance-1 (CRM1) or exportin1, in the carboxyl-terminus third of the protein (15).

The nuclear–cytoplasmic distribution of the huntingtin protein is likely to play an important role in HD progression. Huntingtin localization is affected by cell stress, which triggers N17 phosphorylation leading to its dissociation from the ER and accumulation in the nucleus (3,4). Endogenous huntingtin localizes to nuclear cofilin-actin rods during cell stress, and this stress response is impaired in the presence of polyglutamine-expanded mutant huntingtin (16). Nuclear huntingtin is also known to affect transcriptional regulation, and altered transcription upon polyglutamine expansion is thought to be a key mechanism in HD pathogenesis (17). Compelling evidence also supports the nucleus as a site of mutant huntingtin-mediated toxicity. In cell-based systems, addition of an exogenous nuclear localization signal (NLS) or nuclear export signal (NES) to polyglutamine-expanded amino-terminal huntingtin fragments has opposing effects on cell viability (18,19), whereby nuclear exclusion is beneficial and nuclear localization is toxic. Mutation of methionine residue eight to proline (M8P) disrupts N17 alpha-helical structure and leads to nuclear localization of huntingtin, dramatically increasing the toxicity of the expanded form (4). Similarly, transgenic mice expressing an NLS fused to toxic huntingtin fragments display neurodegenerative phenotypes equivalent to their nonlocalized counterparts (20,21) suggesting that the pathogenicity of these transgenes may be accounted for in large part by the disruption of nuclear processes. In a number of HD mouse models, nuclear accumulation of mutant huntingtin correlates with disease progression (22–32).

In our effort to further characterize the role of the N17 domain in the regulation of huntingtin localization, we noted that its sequence closely resembles the leucine-rich NES (LR-NES) recognized by the nuclear export factor CRM1. We therefore hypothesized that CRM1-mediated nuclear export may contribute to the cytoplasmic retention of N17 fusion proteins observed by our group and others (4,5,14). In this study, we show that N17-mediated cytoplasmic retention is dependent on the hydrophobicity of its NES consensus residues and is sensitive to the CRM1 inhibitor, leptomycin B. N17 physically interacts with CRM1 in a manner dependent on its alpha-helical nature and the presence of RanGTP. We further demonstrate that the nuclear–cytoplasmic distribution of endogenous huntingtin is affected by conditions inhibiting the dissociation of CRM1-cargo in the cytoplasm. Finally, we show that structure-modifying N17 phosphorylation specifies the localization of endogenous huntingtin between the basal body and stalk of the primary cilium. We present the hypothesis that huntingtin can dynamically communicate between the cytoplasm, nucleus and primary cilium, in a signaling-dependent manner, and that this is defective in HD.

RESULTS

N17 contains a potential leucine-rich nuclear export consensus sequence

We have previously shown that while the fusion of the N17 domain to YFP resulted in nuclear exclusion of the fluorescent protein, the L4A mutation resulted in its nuclear accumulation (4). Examination of the evolutionarily conserved N17 amino acid sequence revealed that it corresponds to the leucine-rich NES (LR-NES) recognized by the nuclear export factor CRM1 (33) (Fig. 1). Binding of LR-NESs requires that four of the five consensus hydrophobic residues be spatially coordinated with the five hydrophobic pockets of the NES docking site in CRM1 (33–35). As shown in Figure 1A, N17 fits the NES consensus with two possible alignments according to which either the Φ_3 or Φ_4 position, residue K15 or residue S16, is naturally compromised with respect to hydrophobicity: $L_4\text{-x-x-}L_7\text{-x-x-x-}F_{11}\text{-x-x-x-}\underline{K_{15}}\text{-x-}F_{17}$ or $L_4\text{-x-x-}L_7\text{-x-x-x-}F_{11}\text{-x-x-}L_{14}\text{-x-}\underline{S_{16}}$.

If N17 acts as an LR-NES, then L4A mutation would result in the loss of hydrophobicity at the Φ_0 position (Fig. 1A). We therefore asked whether restoring the hydrophobicity of Φ_3 or Φ_4 in the context of the L4A mutation could restore the four hydrophobic positions required for CRM1 binding and, in turn, nuclear exclusion. As shown in Figure 1B, N17-L4A/S16L-YFP (panel d), but not N17-L4A/K15L-YFP (panel c), displayed predominantly cytoplasmic localization. This suggests that the N17 sequence does in fact behave as an LR-NES and identifies S16 as the Φ_4 residue. Consistent with this, mutation of the Φ_2 residue F11 to alanine in the context L4A/F11A/S16L, once again diminishing the number of hydrophobic consensus residues to three, abolishes nuclear exclusion (Fig. 1B, panel e). Thus, the N17 residues that fit the NES consensus sequence are those displayed in bold type in Figure 1A. The next steps were to test the functional pathway of N17-mediated nuclear export to establish this sequence as a *bone fide* LR-NES.

N17-mediated nuclear exclusion is sensitive to leptomycin B

The *streptomyces* metabolite leptomycin B targets a cysteine residue within the CRM1 NES docking site, covalently modifying and thereby irreversibly inactivating the nuclear export receptor and inhibiting all CRM1-dependent nuclear export (36,37). Leptomycin B is therefore a highly specific and useful tool for studying the requirement of CRM1 for the nuclear exclusion of proteins. Cytoplasmic localization of the huntingtin protein has previously been shown to be sensitive to leptomycin B both as a full-length fluorescent protein fusion (15) and in the context of endogenous huntingtin (38,39). This effect was presumed to be due to the inhibition of CRM1-dependent nuclear export via the carboxyl-terminal NES within the huntingtin protein at position 2404 (15). However, we found that leptomycin B treatment also resulted in nuclear accumulation of an N17–YFP fusion protein (Fig. 2A). These results strongly support the CRM1-dependent
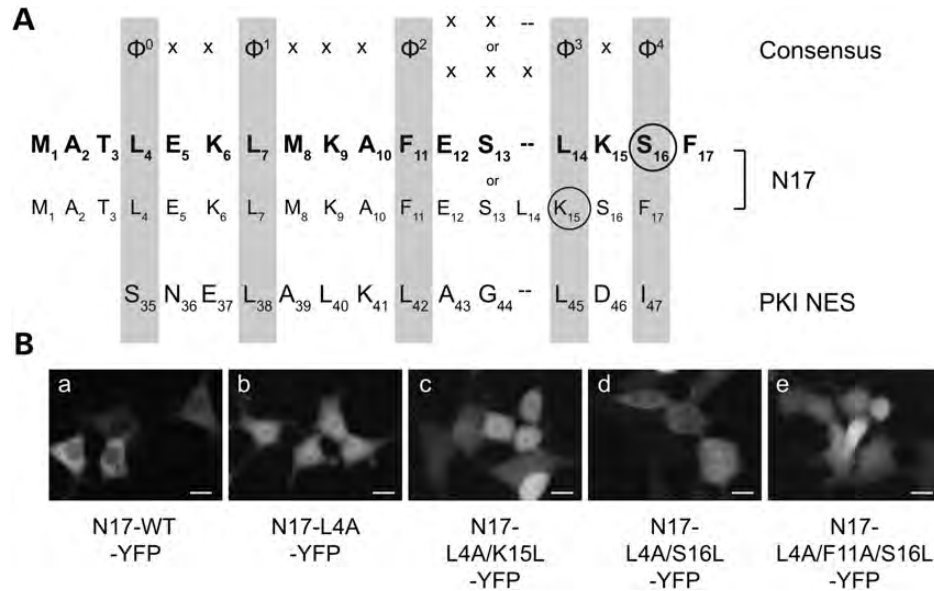
Figure 1. Huntingtin N17 contains a potential conserved CRM1 NES. (**A**) Alignment of the N17 sequence with the LR–NES consensus sequence. (**B**) Representative images of N17 consensus mutants transiently expressed as YFP fusions in HEK 293 cells. Scale bar = 10 μm.

NES activity of the N17 domain. Fusion of the LR-NES canonical protein kinase inhibitor (PKI) NES to YFP was used as a positive control and showed predicted sensitivity to leptomycin B (Fig. 2A, panels a and b) while the PKI-L38A/L42A mutant displayed nuclear localization in the absence of leptomycin B (Fig. 2A, panels c and d). As was previously reported, N17-YFP mutants N17-M8P-YFP (4) (panels g and h) and N17-S13D/S16D-YFP (3) (panels i and j) accumulate in the nucleus even under regular growth conditions. Both of these N17 mutants exhibit loss of alpha-helical content and decreased ER binding (3,4). Conversely, N17-S13A/S16A-YFP displays increased alpha-helicity and enhanced ER binding (3). While this mutant remains localized to the cytoplasm in the absence of leptomycin B, it nonetheless accumulates in the nucleus upon leptomycin B treatment (Fig. 2A, panels k and l).

Leptomycin B does not cause ER stress

We have previously shown that N17-YFP disengages from the ER and accumulates in the nucleus upon induction of the unfolded protein response (UPR) by temperature shift or chemical agents such as tunicamycin and dithiothreitol (4). We were therefore concerned that we may have induced ER stress with leptomycin B treatment and that the observed nuclear accumulation of N17-YFP was due to its passive diffusion into the nucleus upon ER release. It was not previously known if this compound could induce ER stress. We therefore tested whether leptomycin B could induce the ER stress marker Xbox-binding protein 1 (XBP1). In response to ER stress, XBP1 mRNA is spliced to remove a translation inhibition element in the mRNA leading to uninhibited translation and production of the 50 kDa XBP1 transcription factor (40). As shown in Figure 3, while tunicamycin treatment resulted in the XBP1 splicing typical of ER stress, extended leptomycin B treatment did not. Thus the nuclear exclusion mediated by N17 is due to its ability to act as a

CRM1-dependent NES from the nucleus, independent of the status of UPR stress at the ER.

Huntingtin N17 interacts with CRM1

We next asked whether we could detect an interaction between the N17–YFP fusion protein and the nuclear export factor, CRM1. As shown in Figure 4A, N17-YFP co-immunoprecipitated with the Flag-tagged-CRM1 protein upon their co-expression in HEK 293 cells. N17-M8P-YFP and N17-S13D/S16D-YFP mutants, which do not display nuclear exclusion, were not detected in the anti-Flag immunoprecipitations. Conversely, the N17-S13A/S16A-YFP mutant was capable of interacting with Flag-CRM1. These data indicate that N17 interacts with CRM1 in a manner dependent on its alpha-helical nature. An important technical note in this experiment is that the critical Ran gradient is disrupted upon cell lysis, and GTP is rapidly hydrolysed to GDP. Directional transport across the nuclear pore depends on a concentration gradient in which the small GTP-binding Ras family protein, Ran, is GTP-bound in the nucleus and GDP-bound in the cytoplasm (35). In the nucleus, CRM1 requires RanGTP to bind NES-bearing cargo. The ternary complex is transported to the cytoplasm where GTP hydrolysis leads to complex dissociation. The mutant RanQ69L is incapable of exchanging GTP for GDP (41) and therefore inhibits dissociation of the Ran-CRM1-cargo complex in the cytoplasm. Since CRM1 must bind RanGTP to recognize the NES signal in a cargo protein, we required a transient co-expression of a Ran Q69L mutant in order to detect N17-YFP in Flag-CRM1 pull-downs.

N17 has CRM1-dependent NES activity in the context of huntingtin

N17 aligns with the NES consensus (Fig. 1A), confers leptomycin B-sensitive cytoplasmic localization to YFP (Fig. 2) and interacts with CRM1 (Fig. 4). It is theoretically possible,
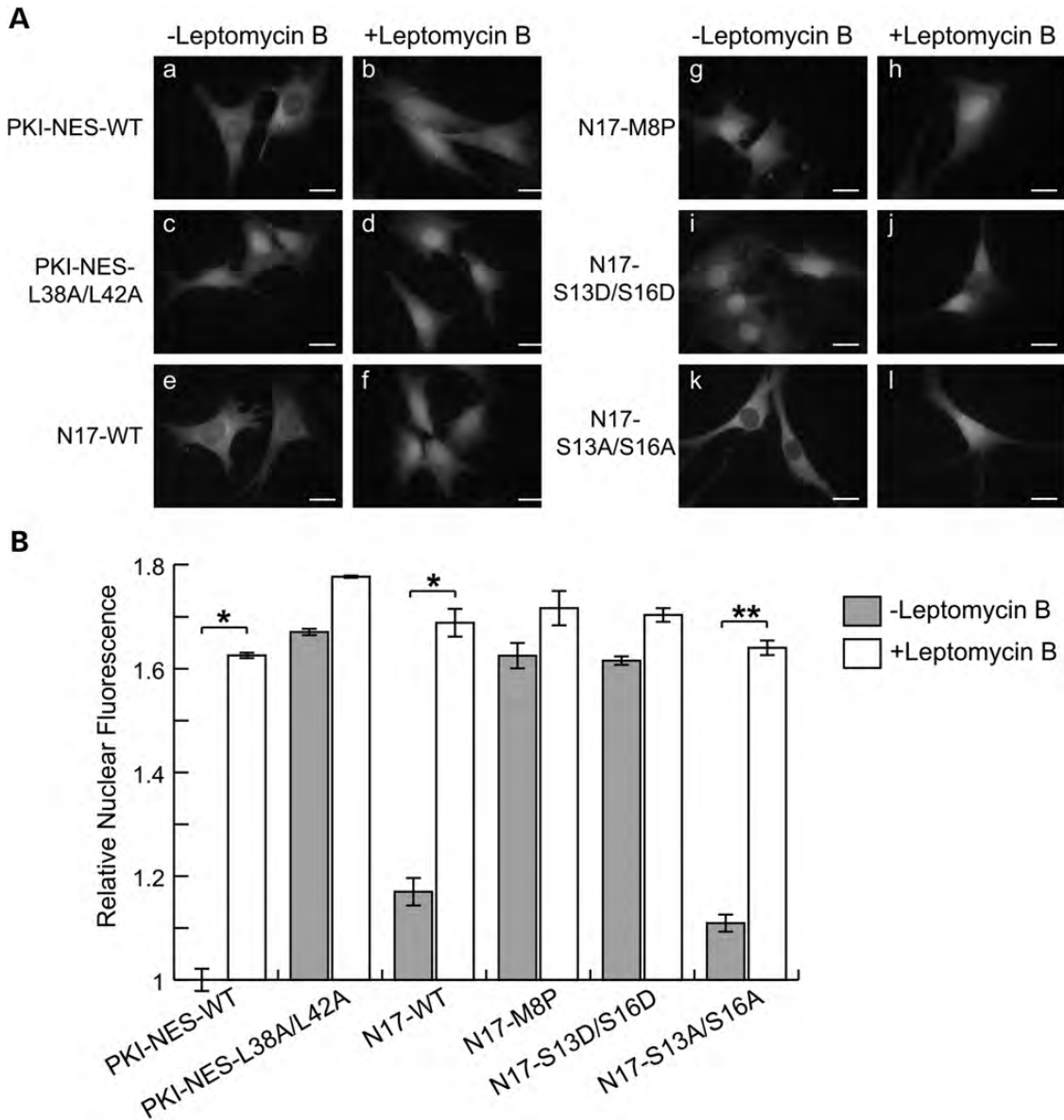
Figure 2. The huntingtin N17 NES is sensitive to leptomycin B. (**A**) ST*Hdh* Q7/Q7 cells stably transfected with YFP fusions of the indicated sequences were imaged after treatment with either vehicle or 10 ng/ml leptomycin B for 30 min. Scale bar = 10 μm. (**B**) The mean percentage nuclear fluorescence was calculated for each condition and normalized to that of the positive control (PKI-WT). Error bars = standard error of the mean for three experiments ($n = 50-100$ cells per condition). *$P < 0.005$; **$P < 0.001$. Scale bar = 10 μm.

however, that in the physical isolation of this domain, we may have uncovered a cryptic activity not biologically relevant in the context of huntingtin. We therefore tested the localization and leptomycin B sensitivity of larger regions of the huntingtin amino terminus. Exon1 of the *IT15* gene encodes the first 81 amino acids of the huntingtin protein, and is thus small enough to enter the nucleus by simple diffusion. This fragment was cloned between the two 26 kDa fluorescent proteins mCerulean and YFP to form mCer-htt-1-81-YFP (Caron *et al.*, 2012, manuscript in preparation). In contrast to the control fusion protein comprising mCer and YFP separated by four glycine residues (mCer-4G-YFP), which can enter the nucleus by diffusion (Fig. 5A, panels a and b), mCer-htt-1-81-YFP displayed cytoplasmic localization under regular

growth conditions (Fig. 5A, panel c). Leptomycin B treatment, however, inhibited nuclear exclusion of mCer-htt-1-81-YFP (Fig. 5A, panel d). Consistent with the localization of the N17-M8P-YFP mutant, mCer-htt-1-81(M8P)-YFP accumulated in the nucleus under both conditions (Fig. 5A, panels e and f). In addition, the larger htt-1-586-YFP fragment exhibited nuclear exclusion that was sensitive to leptomycin B (Fig. 5A, panels g and h). These results show that N17 can behave as a CRM1-dependent NES in a larger context of the huntingtin protein regardless of whether the fluorophore is fused to its amino- or carboxyl-termini. This was consistent with earlier published data that showed that full-length huntingtin could accumulate to the nucleus with a single point mutation in N17 at methionine 8 to proline (4).
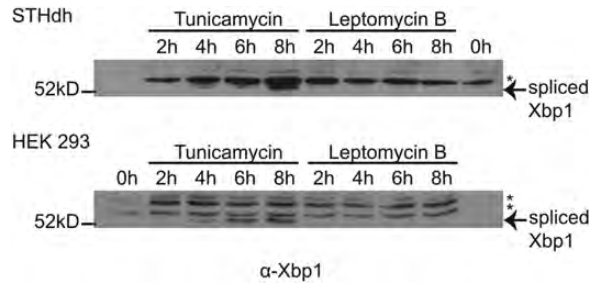
Figure 3. Leptomycin B does not cause the ER UPR. The indicated cell types were treated with either 2 μg/ml tunicamycin or 10 ng/ml leptomycin B for 0–8 h prior to lysis. Equal amounts of protein were separated by SDS–PAGE and immunoblotted with anti-XBP1 antibody. *Non-specific bands.

We next asked whether the N17 domain as part of exon1 could interact with Flag-CRM1. As shown in Figure 5B, mCer-htt-1-81-YFP was co-immunoprecipitated with Flag-CRM1 while the mCer-htt-1-81(M8P)-YFP mutant was not. Thus, we conclude that the N17 sequence has CRM1-dependent nuclear export activity in the context of the huntingtin protein.

Modifying the ran gradient disrupts localization of endogenous huntingtin

Many proteins can artifactually localize to compartments upon over-expression beyond endogenous levels. Transient expression experiments often ignore the effects of altering the stoichiometry of a protein of interest to levels that are not physiologically relevant. To address this, we tested the effect of RanQ69L expression on the localization of endogenous huntingtin. Cells expressing Flag-RanQ69L had reduced nuclear huntingtin staining compared with untransfected cells (Fig. 6A, panel c versus d). This effect was specific to RanQ69L, as transfection of a Flag-tagged control protein did not cause redistribution of endogenous huntingtin (Fig. 6A, panels a, c, e). These observations indicate that huntingtin nuclear localization is regulated by the RanGTP gradient across the nuclear pore complex.

N17 regulates huntingtin localization at the cilia

Huntingtin has recently been shown to regulate the formation of cilia, the sensory or motile organelles that project from many mammalian cell types, and many pathological aspects of an HD mouse model indicate a ciliopathy (42). Additionally, roles for CRM1 and RanGTP in the recruitment and entry of centrosomal and ciliary proteins are rapidly emerging (43–49). The role of huntingtin in cilia function and the effect of N17 phosphorylation on N17-CRM1-RanGTP interaction led us to examine the cilial localization of endogenous huntingtin in its phosphorylated and unmodified states. Cilia projecting from ST*Hdh* cells were identified by immunofluorescence against acetylated tubulin (Fig. 7, panels a and d). Cells were co-stained with antibodies against either unmodified N17 (Fig. 7, panels a–c) or phosphorylated N17 (Fig. 7, panels d–f). The results revealed markedly distinct localization patterns, whereby unmodified huntingtin was found within cilia and N17-phosphorylated huntingtin accumulated

at the ciliary base/centrosome. These data indicated that N17 dephosphorylation corresponded to cilial huntingtin, and/or that N17 phosphorylation could take place after cilial export.

DISCUSSION

In this study, we propose an additional role for the N17 domain in the regulation of huntingtin subcellular localization, once released from the ER. Previous work in our laboratory has established N17 as a membrane-binding domain mediating ER localization (4), and has revealed that N17 residues S13 and S16 undergo CK2-dependent phosphorylation upon cell stress leading to the release of huntingtin from the ER and its accumulation in the nucleus (3,4). The observations described here indicate that N17 also acts as an NES in a manner dependent on its alpha-helical content and the hydrophobicity of its NES consensus residues, and interacts with the nuclear exporter CRM1 in a Ran-dependent manner. This gives rise to a mechanism by which stress-mediated post-translational modification of N17 not only allows its release from the ER, but also promotes nuclear retention of huntingtin by preventing its interaction with CRM1 (see model Fig. 8). This would transiently increase nuclear huntingtin levels to allow huntingtin activity on transcription modulation related to a transient stress response. Post-stress, de-phosphorylation of N17 would presumably be required to allow CRM1 interaction, hence nuclear export and the restoration of huntingtin nuclear levels to steady state. The inability to recover the phospho-mimetic mutant N17-S13D/S16D-YFP in Flag-CRM1 co-immunoprecipitations is consistent with this hypothesis. Additionally, the sensitivity of N17-S13A/S16A-YFP to leptomycin B indicates that N17-mediated huntingtin ER localization can be affected by other factors, and that while N17 phosphorylation may promote ER disengagement, it may not be the only way to trigger ER release.

Post-translational modifications or mutations affecting N17 alpha-helical content, which regulate nuclear-cytoplasmic shuttling (Figs 2 and 5A) (4), also impinge on the toxicity of mutant huntingtin. Recent research suggests that phosphorylation of S13 and S16 leads to increased nuclear localization of huntingtin and concomitant decreased toxicity of the polyglutamine-expanded form (3,10,11). This appears to be at odds with the extensive evidence of increased levels of nuclear mutant huntingtin compared with wild-type huntingtin in HD mouse models (24,50). The selective appearance of nuclear mutant huntingtin in the specific subset of neurons affected in HD strongly implicates the nucleus as a site of mutant huntingtin toxicity. This is supported by the opposing effects of nuclear targeting versus nuclear exclusion of polyglutamine-expanded huntingtin in cell-based and transgenic mouse models (18–21).

In light of these results, how do we reconcile the concurrent increased nuclear localization and decreased toxicity upon phosphorylation of serines 13 and 16? The most parsimonious explanation is that phosphorylation of N17 confers on huntingtin a nontoxic conformation within the nucleus. In contrast, the alpha helix-disrupting mutation M8P, which also leads to nuclear accumulation, likely, confers a toxic conformation (4).

Mutant huntingtin has lower levels of N17 phosphorylation than wild-type huntingtin (3). Based on the current work,
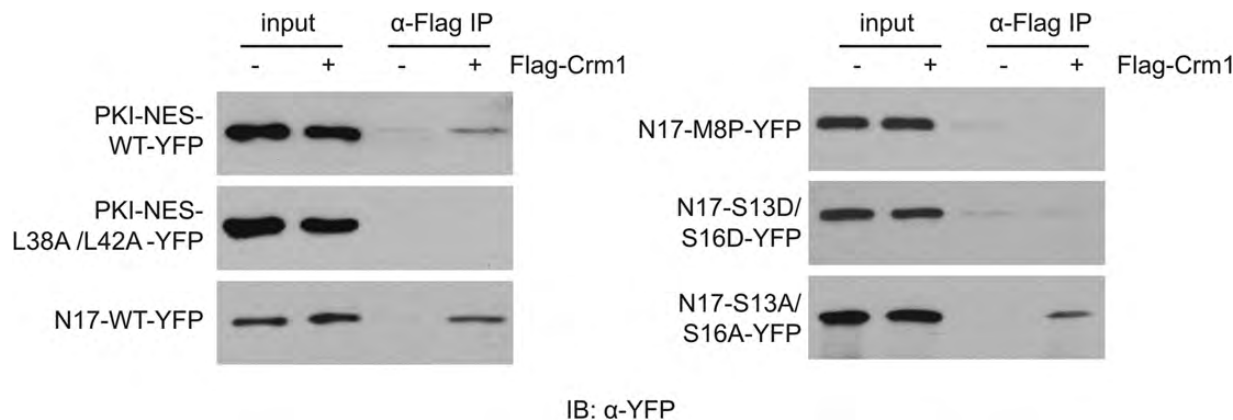
Figure 4. N17 can bind CRM1 in the presence of RanGTP. Human HEK 293 cells were transiently transfected with the indicated YFP fusion proteins and either empty vector (−) or Flag-CRM1 and RanQ69L (+). Cell lysates were incubated with anti-Flag affinity gel (α-Flag IP). After washing, resin-associated proteins were separated by SDS–PAGE and immunoblotted with anti-YFP antibody.

mutant huntingtin would therefore be predicted to interact more strongly with CRM1 and display decreased nuclear localization due to more nuclear export. This too is at odds with the historically observed increased relative levels of nuclear mutant huntingtin. It is possible that while mutant huntingtin can interact better with CRM1, the inherent reduced solubility of polyglutamine-expanded huntingtin prevents proper nuclear export. Alternatively, as N17 phosphorylation is likely sterically hindered by the polyglutamine expansion only two amino acids away on the alpha carbon backbone, so may be the de-phosphorylation of polyglutamine-expanded huntingtin in subnuclear puncta, thus whatever small amount of mutant huntingtin that does get signaled to the nucleus may not be properly de-phosphorylated, and thus progressively accumulates in the nucleus, to potentially nucleate aggregation. Further experiments are required to determine whether polyglutamine expansion affects CRM1 interaction and whether the resulting altered nuclear-cytoplasmic distribution affects the toxicity of the mutant form. What we suggest from this and prior work is that the conformation(s) and resulting activity of the subnuclear population of mutant huntingtin may be of greater importance than the nuclear–cytoplasmic distribution of the entire huntingtin population.

Previously published work from others concluded that the huntingtin N17 domain had an NES activity that was both CRM1 and Ran independent (13). However, in the 6 years since that study was published, the role of TPR has been shown to be increasingly important for mRNA export (51), and knock down of TPR has been shown to cause cell senescence (52). Unlike our study, the previous study did not use leptomycin B treatment, but like our study, did use Ran Q69L expression in HEK 293 cells, however at times and levels that resulted in dead cells in our hands. Additionally, no N17 mutants or critical residues were defined, and no attempt was made to validate the proposed mechanism to full-length huntingtin. Additionally, TPR has been shown by others to be a critical interactor of CRM1 for nuclear export, but in a classical Ran-dependent manner (53).

In addition to their well-known roles in nuclear–cytoplasmic transport, RanGTP and CRM1 control the spatial coordination of proteins to specific loci during mitosis (54). CRM1 has also been identified at centrosomes in a number of model systems and its interaction with specific NES-containing proteins can regulate their impact on centrosome duplication (43,55,56). CRM1 NES binding is required for the proper localization of centrosomal proteins centrin and pericentrin (57) and breast cancer 2 susceptibility protein (BRCA2) (58,59). In these cases, this requirement was not necessarily distinguished from CRM1's nuclear export function. An additional layer of complexity has emerged, however, with the evidence that centrosomally located Crm1 directly recruits nucleophosmin (43) and BRCA1 (55) proteins via their NESs. Two independent groups, including ours, have identified endogenous huntingtin at centrosomes, on chromatin undergoing condensation, and on tubulin spindle fibers during mitotic spindle formation and huntingtin has an essential role in spindle orientation during mitosis (3,60). N17-mediated CRM1/RanGTP interaction may play a role in the recruitment of huntingtin to these mitotic structures. Since the huntingtin we detect at these structures is predominantly phosphorylated at serines 13 and 16, it is possible that N17 phosphorylation affects the dissociation of huntingtin from the CRM1/RanGTP complex following its recruitment. It is also possible that the huntingtin carboxyl-terminal NES may play a role in its recruitment to these structures. Some large scaffolding proteins can contain multiple nuclear import and export signals, such as the 100 kDa alpha catenin protein, and one of these export signals can be inhibited by protein–protein interactions to regulate the rate of dynamics between organelles (61).

Huntingtin has been shown to play a role in the regulation of cilia, organelles projected from specialized centrosomes that have sensory or motile functions. HD knock-in mice and HD patient samples display abnormal ciliation of brain ventricles, and in mice this is associated with asynchronous beating of the cilia and abnormal flow of the cerebrospinal fluid (42). However, striking similarities between the physical and molecular nature of nuclear and ciliary transport machinery are emerging (49). RanGTP accumulation at basal bodies is linked to ciliogenesis through the targeting of certain ciliary proteins and RanGTP has been proposed to regulate the recruitment and release of binding partners to ciliary elements (45–48).
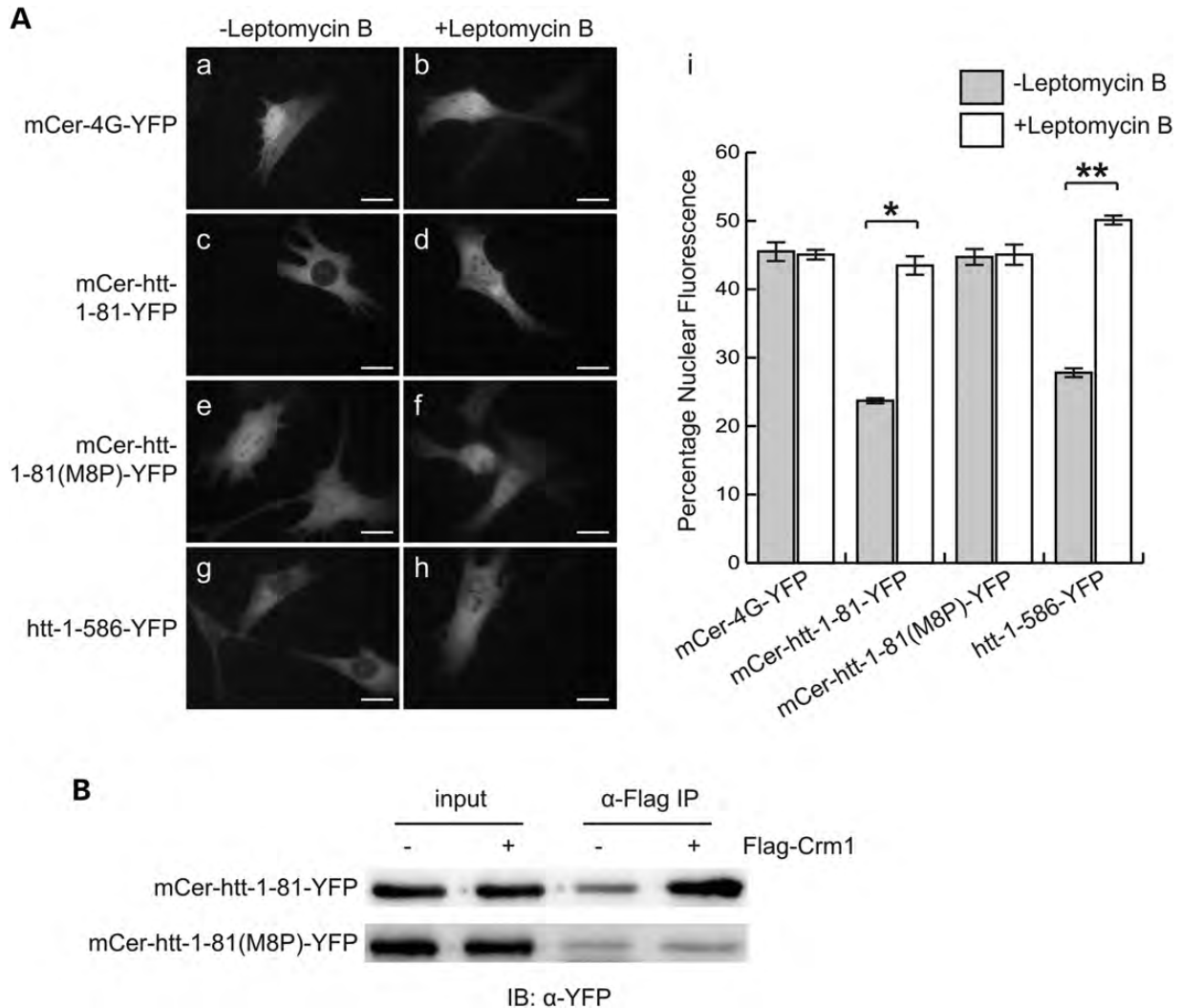
Figure 5. N17 functions as an NES in the context of a huntingtin fragment. (**A**) ST*Hdh* Q7/Q7 cells transiently transfected with the indicated constructs were imaged after treatment with either vehicle or 10 ng/ml leptomycin B for 60 min. The mean percentage nuclear fluorescence was calculated for each condition. Error bars = standard error of the mean for three experiments ($n = 50–100$ cells per condition). *$P < 0.005$; **$P < 0.001$. Scale bar = 10 μm. (**B**) Human HEK 293 cells were transiently transfected with the indicated YFP fusion proteins and co-immunoprecipitation with Flag-CRM1 was performed as in Figure 4.

Recently, we have described the presence of a karyopherin beta2 or transportin-dependent 'PY-NLS' in huntingtin between amino acids 172 and 202 (62). This NLS has the ability to mediate nuclear entry by either the importin/karypherin beta1 or the transportin/karyopherin beta2 pathways. The karyopherin beta2 nuclear transport factor is known to be able to mediate the entry of the retinitis pigmentosa 2 (48) and KIF17 proteins (45) across the primary cilial barrier into the primary cilium. Cilial entry of KIF17 requires a nuclear localization sequence and another undefined domain (45), our data indicate that the huntingtin NLS/CLS at 172-202 is regulated by N17 phosphorylation for both nuclear and cilial entry. The role of the Ran gradient across the cilial barrier and the use of nuclear import factors (45) and nucleoporins to mediate cilial entry (32) suggest that nuclear export factors like CRM1 may also be used in cilia to mediate cilial export and that the two organelles share a common mechanism of localization and regulation, as recently suggested by others (63).

In summary, the N17 domain of huntingtin is a multifunctional localization signal that regulates the subcellular localization of huntingtin, is regulated by post-translational modification and contributes to the pathogenic mechanism by which the mutant protein causes disease. Huntingtin is now seen as a dynamic scaffolding protein that can be signaled to the nucleus, cytoplasm or motor protein complexes in the cytoplasm and the primary cilium. All of these locations are critical to the normal biology of a striatal neuron for interneuronal communication, and thus mislocalization may explain the specificity of neuronal pathology in HD. This current work extends our understanding of the factors contributing to this complex process and ultimately directs our focus toward N17 as a viable target in the pursuit of the development of effective treatments for HD.
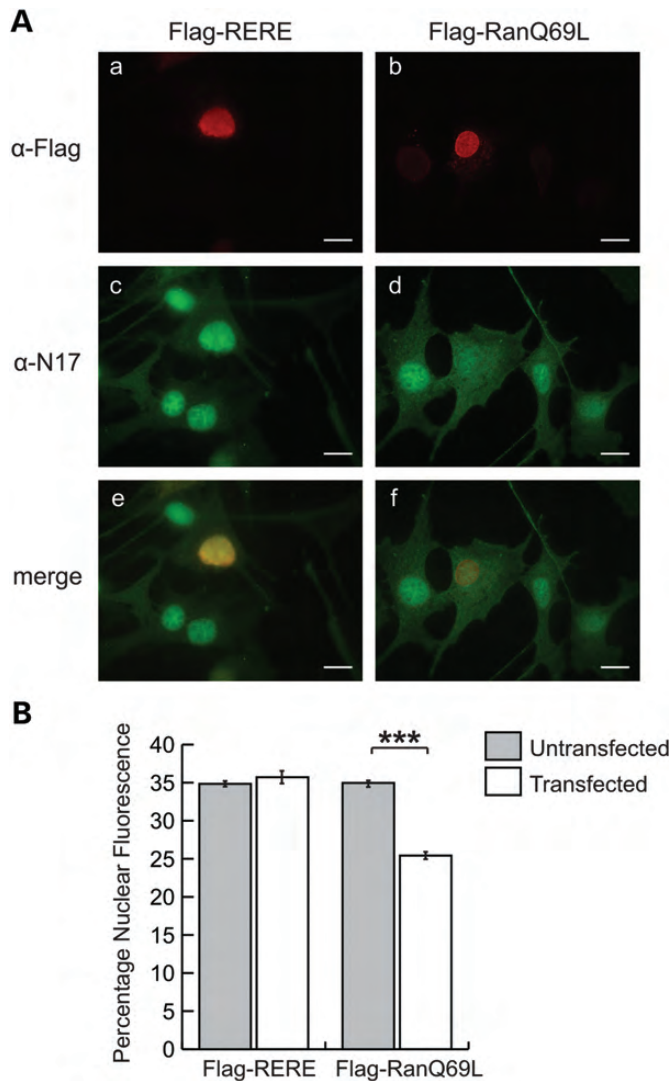
A

B

Figure 6. Disrupting the Ran gradient affects the nuclear localization of endogenous full-length huntingtin. (**A**) ST*Hdh* cells were transiently transfected with Flag-RERE or Flag-RanQ69L and immunofluorescence performed against the Flag epitope tag (α-flag, red) and endogenous huntingtin (α-N17, green). Scale bar = 10 μm. (**B**) The mean percentage nuclear fluorescence was calculated for untransfected and transfected cells. Error bars = standard error of the mean for three experiments ($n = 50–100$ cells per condition). ***$P < 0.00002$.

MATERIALS AND METHODS

Antibodies and imaging reagents

Leptomycin B, anti-Flag M2 antibody and affinity gel, GTP, GTP-γ-S, tunicamycin, puromycin, Hoechst stain, paraformaldehyde, NP40, fetal bovine serum (FBS) and cloning discs were from Sigma-Aldrich. Sodium dodecyl sulfate (SDS) loading buffer and Turbofect transfection reagent were from Fermentas. Anti-XBP1 antibody was from Santa Cruz Biotechnology Inc (sc-7160), anti-YFP antibody from Clontech, anti-N17 antibody was prepared as previously published (3) and AlexaFluor secondary antibodies were from Molecular Probes. Protease inhibitor cocktail was from Roche.

Plasmid expression constructs

peYFPN1-htt[1-586], peYFPN1-N17 and M8P, S13D/S16D and S13A/S16A mutants have been previously described (3,4). peYFPN1-N17-L4A and L4A/K15L, L4A/S16L and L4A/F11A/S16L mutants were generated by inverse PCR amplification of the peYFPN1-N17 plasmid with primers encoding the appropriate mutations and subsequent ligation. peYFPC1-PKI NES and peYFPC1-PKI NES-L38A/L42A were generated by annealing synthetic oligos (PKI NES: CCGGAAGCAAT GAATTAGCCTTGAAATTAGCAGGTCTTGATATCTAG and GTACCTAGATATCAAGACCTGCTAATTTCAAGGC TAATTCATTGCTT; PKI NES-L38A/L42A: CCGGAAG CAATGAAGCAGCCTTGAAAGCAGCAGGTCTTGATAT CTAG and GTACCTAGATATCAAGACCTGCTGCTTT CAAGGCTGCTTCATTGCTT) and ligation into the peYFPC1 vector (Clontech). p3XFlagCMV10-hCRM1 is Addgene plasmid 17647 (43). Untagged RanQ69L used in CRM1 co-immunoprecipitations was generated by PCR amplification of the RanQ69L cDNA, including stop codon, from pGEX-5X1-RanQ69L (64) and ligation into peYFPN1 (Clontech) to give RanQ69L-stop-YFP. Flag-RanQ69L was generated by PCR amplification of the RanQ69L cDNA from pGEX-5X1-RanQ69L (64) and ligation into p3XFlag-CMV10 vector (Sigma). mCer-4G-YFP, mCer-htt-1-81-YFP and mCer-htt-1-81(M8P)-YFP are described elsewhere (Caron *et al.*, 2012, manuscript in preparation). The Flag-RERE (481-1566) vector is described elsewhere (65).

Cell culture and transfection

HEK 293 cells were cultured in alpha-minimal essential media containing 10% FBS at 37°C with 5% CO_2. ST*Hdh* striatal cells were cultured as described previously (66). ST*Hdh* cell lines stably expressing PKI-YFP, PKI-L38A/L42A-YFP, N17-YFP, N17-M8P-YFP, N17-S13D/S16D-YFP and N17-S13A/S16A-YFP were generated by co-transfecting the respective plasmids and the Puro1 plasmid conferring puromycin resistance at a 10:1 molar ratio using Turbofect according to manufacturer's directions. Transfected cells were grown in media containing 10 μg/ml puromycin and single colonies transferred to individual plates with cloning discs. Multiple clones were used in experiments to ensure phenotypic consistency. Transient transfection of HEK 293 and ST*Hdh* cells was by Turbofect according to manufacturer's directions.

Cell fixation and immunofluorescence

Cells expressing YFP fusion proteins were fixed with freshly prepared 4% (w/v) paraformaldehyde in PBS at room temperature for 15 min and nuclei counterstained with Hoechst dye for 15 min at room temperature prior to imaging in PBS. For immunofluorescence, cells were fixed with freshly prepared 4% (w/v) paraformaldehyde in PBS at room temperature for 15 min, permeabilized with 0.5% Triton X-100 and 1% FBS in PBS at 4°C for 12 min and non-specific binding was blocked with 2% FBS in PBS for 1 h at room temperature. Antibodies were diluted in antibody dilution buffer (1% FBS and 0.02% Tween-20 in PBS) and incubated with cells as follows: anti-Flag (1:1000) 2 h at room temperature,
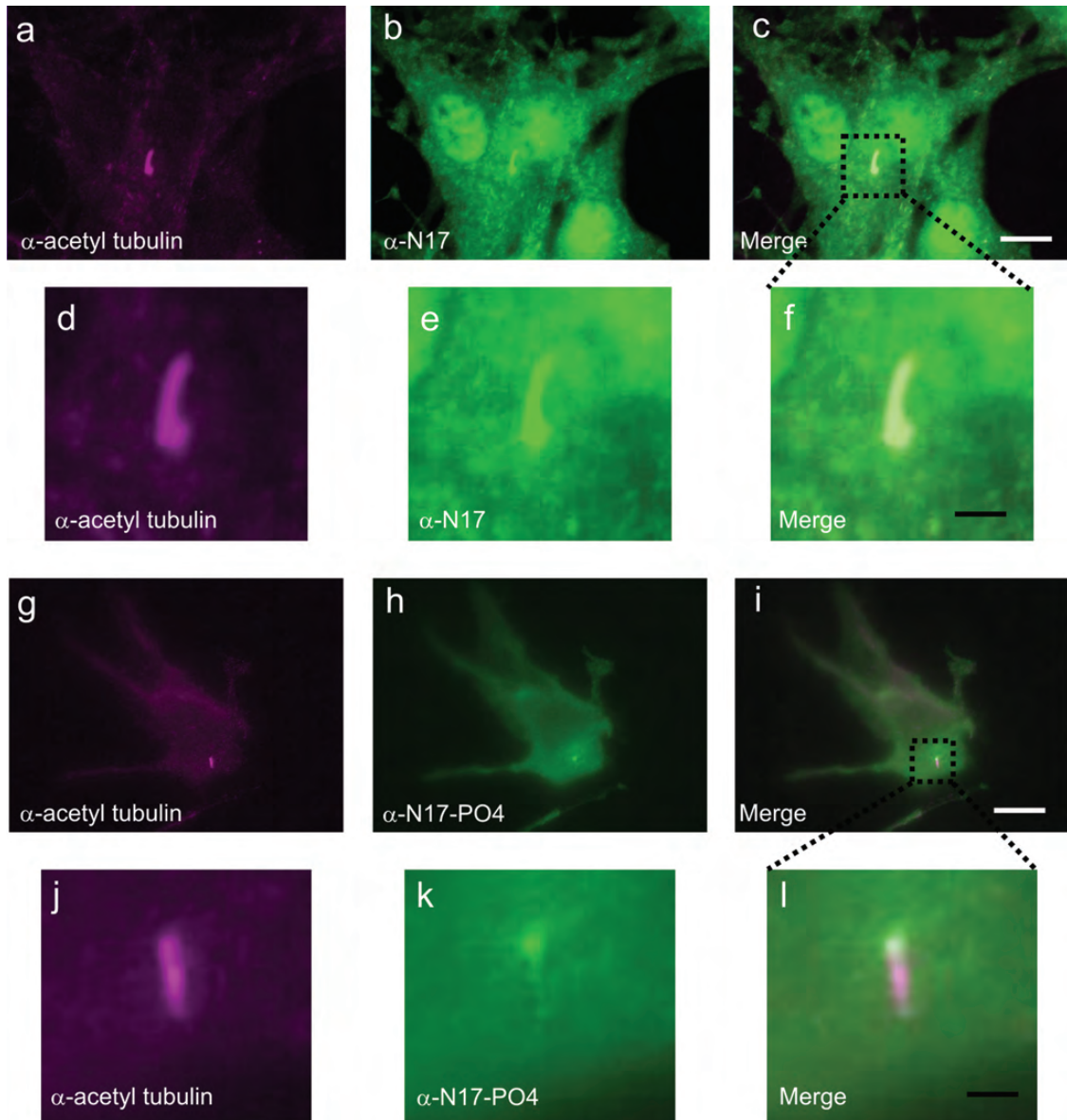
Figure 7. N17 phosphorylation specifies huntingtin localization between the base and stalk of the primary cilium. Co-immunofluorescence on ST*Hdh* $^{Q7/Q7}$ cells was performed against acetylated tubulin to locate cilia (magenta; a, d, g, j) and either unmodified N17 (b and e) or phosphorylated N17 endogenous huntingtin (h and k). Magnified inset images show localization of unmodified N17 primarily to the cilia stalk (d−f) and phosphorylated N17 huntingtin to the basal body (j−l). White scale bars are 10 μm. Black scale bars are 2 μm. Merged magenta−green signal appears as white in (c, f, i, l).

AlexaFluor 594 goat α-mouse (1:1000) 1 h at room temperature, anti-N17 (1:500) overnight at 4°C, AlexaFluor 488 donkey α-rabbit (1:1000) 1 h at room temperature. Cells were washed three times with PBS between each antibody incubation and nuclei counterstained with Hoechst dye for 15 min at room temperature prior to imaging in PBS.

Imaging and calculation of percentage nuclear fluorescence

Imaging was performed using a Nikon TE200 inverted widefield epifluorescence microscope and plan apochromat ×60 oil immersion objective (Nikon, Japan). The imaging platform controlling the scope was NIS elements 3.1. All filter sets and dichroic filters were from Semrock (Rochester, NY, USA) and the filter wheel was from Sutter Instruments (Novato, CA, USA). The light source was a 175 W Xenon lap (Sutter Instruments), with ND2 or ND4 filters. Images were acquired using a Hamamatsu Orca ER digital camera (Hamamatsu Photonics, Japan).

For cells expressing YFP fusion proteins, percentage nuclear fluorescence was calculated using Cell Profiler (www.cellprofiler.org) (67). Briefly, images of Hoechst-stained nuclei were used to define nuclear area and corresponding cell area identified in YFP images. YFP fluorescence intensity was calculated for nuclear and whole cell area and the percentage nuclear fluorescence calculated using the equation: percentage nuclear fluorescence = (nuclear intensity/
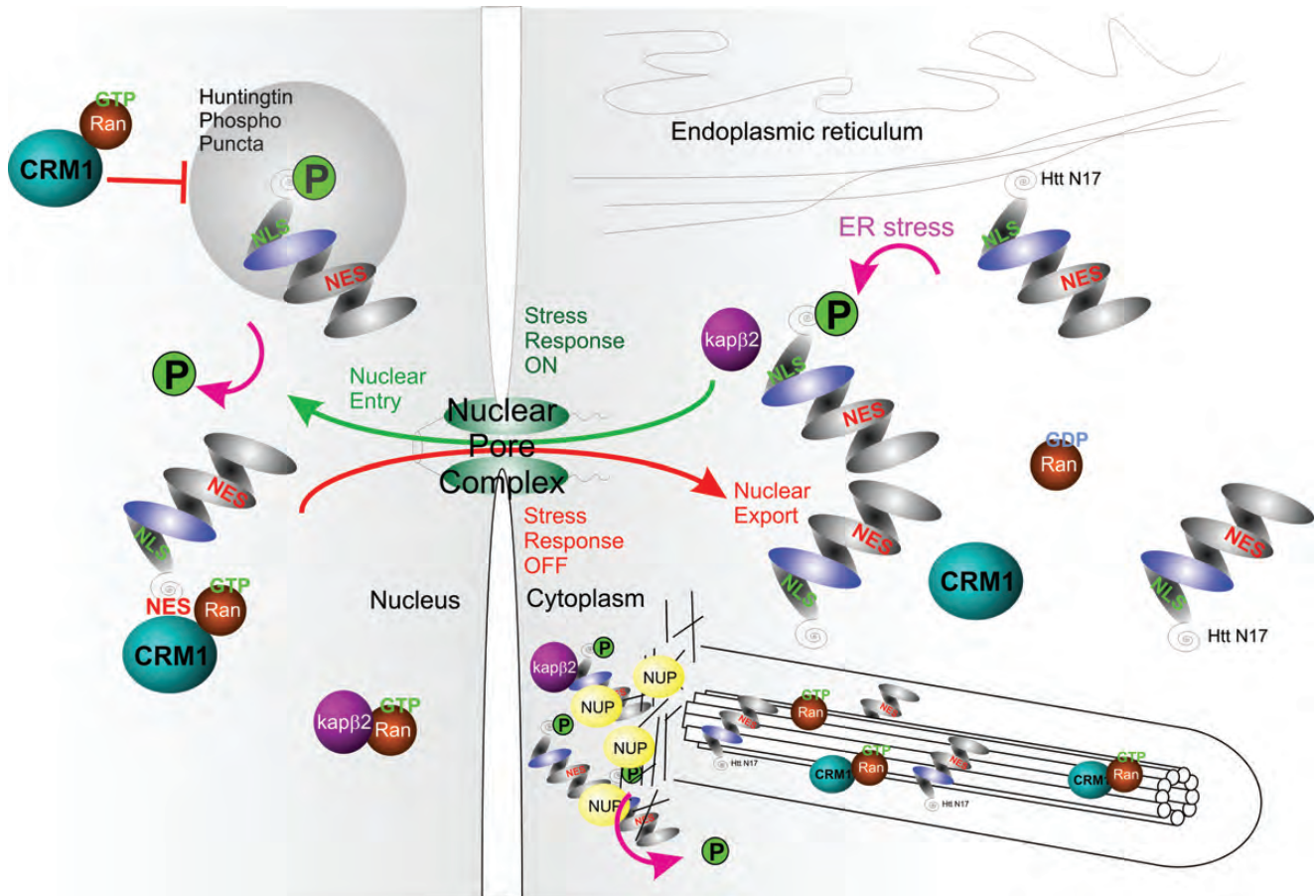
Figure 8. Model of the role of the multifunctional N17 in huntingtin stress response. Upon ER stress or other signaling, huntingtin N17 is phosphorylated and this allows release from the ER to enter the nucleus or primary cilium via karyopherin beta2. Once in the nucleus, phospho-N17 huntingtin localizes to huntingtin chromatin-dependent nuclear puncta, where the interaction of the N17 NES with CRM1/RanGTP is occluded by phosphorylation. Upon de-phosphorylation post-stress, the NES is exposed to the CRM1/RanGTP complex and huntingtin is exported out of the nucleus. With mutant huntingtin, N17 is sterically hindered by the polyglutamine expansion, causing either poor phosphorylation of N17 to inhibit the stress response, and/or poor de-phosphorylation of nuclear mutant huntingtin resulting in nuclear accumulation and lack of proper control of the stress response. Phospho-N17 huntingtin is seen at the basal body, but not within the cilium, suggesting that a complex with CRM1 and RanGTP can mediate huntingtin export from the cilium in a mechanism identical to nuclear export.

whole cell intensity) × 100. For cells analyzed by anti-Flag/anti-N17 immunofluorescence, the percentage nuclear fluorescence of untransfected and transfected cells was quantified using Simple PCI (Compix). Briefly, nuclear and whole cell intensities were collected by manually defining the nuclear and whole cell regions in each image, then collecting blank areas of equal size to represent the image background. The intensities of the defined regions were then measured using the Simple PCI measurement tool. The percentage nuclear fluorescence was calculated using the equation: percentage nuclear fluorescence = [(nuclear intensity-background)/(whole cell intensity-background)] × 100.

CRM1 co-immunoprecipitation

HEK 293 cells were co-transfected with YFP fusion proteins, Flag-CRM1 and untagged RanQ69L as indicated in figure legends. Seventy-two hours post-transfection, cells were lysed in NP40 lysis buffer (50 mM Tris–HCl, pH 8.0, 150 mM NaCl, 1% NP40, protease inhibitor cocktail) containing 2 mM GTP-γ-S for 15 min on ice and lysates cleared by centrifugation. Supernatants were incubated with anti-Flag affinity beads in NP40 lysis buffer containing 10 mM GTP for 30 min with rotation at 4°C. Affinity beads were washed three times with ice-cold PBS containing 2 mM GTP. Purified proteins were eluted with SDS loading buffer at 95°C for 10 min prior to separation by SDS–PAGE and immunoblotting.

Conflict of Interest statement. None declared.

REFERENCES

1. The Huntington's Disease Collaborative Research Group. (1993) A novel gene containing a trinucleotide repeat that is expanded and unstable on Huntington's disease chromosomes. *Cell*, **72**, 971–983.
2. Kim, M.W., Chelliah, Y., Kim, S.W., Otwinowski, Z. and Bezprozvanny, I. (2009) Secondary structure of Huntingtin amino-terminal region. *Structure*, **17**, 1205–1212.
3. Atwal, R.S., Desmond, C.R., Caron, N., Maiuri, T., Xia, J., Sipione, S. and Truant, R. (2011) Kinase inhibitors modulate huntingtin cell localization and toxicity. *Nat. Chem. Biol.*, **7**, 453–460.
4. Atwal, R.S., Xia, J., Pinchev, D., Taylor, J., Epand, R.M. and Truant, R. (2007) Huntingtin has a membrane association signal that can modulate huntingtin aggregation, nuclear entry and toxicity. *Hum. Mol. Genet.*, **16**, 2600–2615.
5. Rockabrand, E., Slepko, N., Pantalone, A., Nukala, V.N., Kazantsev, A., Marsh, J.L., Sullivan, P.G., Steffan, J.S., Sensi, S.L. and Thompson, L.M. (2007) The first 17 amino acids of Huntingtin modulate its sub-cellular localization, aggregation and effects on calcium homeostasis. *Hum. Mol. Genet.*, **16**, 61–77.
6. Dlugosz, M. and Trylska, J. (2011) Secondary structures of native and pathogenic huntingtin N-terminal fragments. *J Phys Chem B*, **115**, 11597–11608.
7. Aiken, C.T., Steffan, J.S., Guerrero, C.M., Khashwji, H., Lukacsovich, T., Simmons, D., Purcell, J.M., Menhaji, K., Zhu, Y.Z., Green, K. *et al.* (2009) Phosphorylation of threonine 3: implications for Huntingtin aggregation and neurotoxicity. *J. Biol. Chem.*, **284**, 29427–29436.
8. Thompson, L.M., Aiken, C.T., Kaltenbach, L.S., Agrawal, N., Illes, K., Khoshnan, A., Martinez-Vincente, M., Arrasate, M., O'Rourke, J.G., Khashwji, H. *et al.* (2009) IKK phosphorylates Huntingtin and targets it for degradation by the proteasome and lysosome. *J. Cell Biol.*, **187**, 1083–1099.
9. Steffan, J.S., Agrawal, N., Pallos, J., Rockabrand, E., Trotman, L.C., Slepko, N., Illes, K., Lukacsovich, T., Zhu, Y.Z., Cattaneo, E. *et al.* (2004) SUMO modification of Huntingtin and Huntington's disease pathology. *Science*, **304**, 100–104.
10. Gu, X., Greiner, E.R., Mishra, R., Kodali, R., Osmand, A., Finkbeiner, S., Steffan, J.S., Thompson, L.M., Wetzel, R. and Yang, X.W. (2009) Serines 13 and 16 are critical determinants of full-length human mutant huntingtin induced disease pathogenesis in HD mice. *Neuron*, **64**, 828–840.
11. Di Pardo, A., Maglione, V., Alpaugh, M., Horkey, M., Atwal, R.S., Sassone, J., Ciammola, A., Steffan, J.S., Fouad, K., Truant, R. *et al.* (2012) Ganglioside GM1 induces phosphorylation of mutant huntingtin and restores normal motor behavior in Huntington disease mice. *Proc. Natl Acad. Sci. USA*, **109**, 3528–3533.
12. Orr, A.L., Li, S., Wang, C.E., Li, H., Wang, J., Rong, J., Xu, X., Mastroberardino, P.G., Greenamyre, J.T. and Li, X.J. (2008) N-terminal mutant huntingtin associates with mitochondria and impairs mitochondrial trafficking. *J. Neurosci.*, **28**, 2783–2792.
13. Cornett, J., Cao, F., Wang, C.E., Ross, C.A., Bates, G.P., Li, S.H. and Li, X.J. (2005) Polyglutamine expansion of huntingtin impairs its nuclear export. *Nat. Genet.*, **37**, 198–204.
14. Yan, Y., Peng, D., Tian, J., Chi, J., Tan, J., Yin, X., Pu, J., Xia, K. and Zhang, B. (2011) Essential sequence of the N-terminal cytoplasmic localization-related domain of huntingtin and its effect on huntingtin aggregates. *Sci. China Life Sci.* **54**, 342–350.
15. Xia, J., Lee, D.H., Taylor, J., Vandelft, M. and Truant, R. (2003) Huntingtin contains a highly conserved nuclear export signal. *Hum. Mol. Genet.*, **12**, 1393–1403.
16. Munsie, L., Caron, N., Atwal, R.S., Marsden, I., Wild, E.J., Bamburg, J.R., Tabrizi, S.J. and Truant, R. (2011) Mutant huntingtin causes defective actin remodeling during stress: defining a new role for transglutaminase 2 in neurodegenerative disease. *Hum. Mol. Genet.*, **20**, 1937–1951.
17. Cha, J.H. (2007) Transcriptional signatures in Huntington's disease. *Prog. Neurobiol.*, **83**, 228–248.
18. Peters, M.F., Nucifora, F.C. Jr, Kushi, J., Seaman, H.C., Cooper, J.K., Herring, W.J., Dawson, V.L., Dawson, T.M. and Ross, C.A. (1999) Nuclear targeting of mutant Huntingtin increases toxicity. *Mol. Cell Neurosci.*, **14**, 121–128.
19. Saudou, F., Finkbeiner, S., Devys, D. and Greenberg, M.E. (1998) Huntingtin acts in the nucleus to induce apoptosis but death does not correlate with the formation of intranuclear inclusions. *Cell*, **95**, 55–66.
20. Benn, C.L., Landles, C., Li, H., Strand, A.D., Woodman, B., Sathasivam, K., Li, S.H., Ghazi-Noori, S., Hockly, E., Faruque, S.M. *et al.* (2005) Contribution of nuclear and extranuclear polyQ to neurological phenotypes in mouse models of Huntington's disease. *Hum. Mol. Genet.*, **14**, 3065–3078.
21. Schilling, G., Savonenko, A.V., Klevytska, A., Morton, J.L., Tucker, S.M., Poirier, M., Gale, A., Chan, N., Gonzales, V., Slunt, H.H. *et al.* (2004) Nuclear-targeting of mutant huntingtin fragments produces Huntington's disease-like phenotypes in transgenic mice. *Hum. Mol. Genet.*, **13**, 1599–1610.
22. Hodgson, J.G., Agopyan, N., Gutekunst, C.A., Leavitt, B.R., LePiane, F., Singaraja, R., Smith, D.J., Bissada, N., McCutcheon, K., Nasir, J. *et al.* (1999) A YAC mouse model for Huntington's disease with full-length mutant huntingtin, cytoplasmic toxicity, and selective striatal neurodegeneration. *Neuron*, **23**, 181–192.
23. Laforet, G.A., Sapp, E., Chase, K., McIntyre, C., Boyce, F.M., Campbell, M., Cadigan, B.A., Warzecki, L., Tagle, D.A., Reddy, P.H. *et al.* (2001) Changes in cortical and striatal neurons predict behavioral and electrophysiological abnormalities in a transgenic murine model of Huntington's disease. *J. Neurosci.*, **21**, 9112–9123.
24. Li, H., Li, S.H., Johnston, H., Shelbourne, P.F. and Li, X.J. (2000) Amino-terminal fragments of mutant huntingtin show selective accumulation in striatal neurons and synaptic toxicity. *Nat. Genet.*, **25**, 385–389.
25. Lin, C.H., Tallaksen-Greene, S., Chien, W.M., Cearley, J.A., Jackson, W.S., Crouse, A.B., Ren, S., Li, X.J., Albin, R.L. and Detloff, P.J. (2001) Neurological abnormalities in a knock-in mouse model of Huntington's disease. *Hum. Mol. Genet.*, **10**, 137–144.
26. Menalled, L.B., Sison, J.D., Dragatsis, I., Zeitlin, S. and Chesselet, M.F. (2003) Time course of early motor and neuropathological anomalies in a knock-in mouse model of Huntington's disease with 140 CAG repeats. *J. Comp. Neurol.*, **465**, 11–26.
27. Menalled, L.B., Sison, J.D., Wu, Y., Olivieri, M., Li, X.J., Li, H., Zeitlin, S. and Chesselet, M.F. (2002) Early motor dysfunction and striosomal distribution of huntingtin microaggregates in Huntington's disease knock-in mice. *J. Neurosci.*, **22**, 8266–8276.
28. Schilling, G., Becher, M.W., Sharp, A.H., Jinnah, H.A., Duan, K., Kotzuk, J.A., Slunt, H.H., Ratovitski, T., Cooper, J.K., Jenkins, N.A. *et al.* (1999) Intranuclear inclusions and neuritic aggregates in transgenic mice expressing a mutant N-terminal fragment of huntingtin. *Hum. Mol. Genet.*, **8**, 397–407.
29. Tallaksen-Greene, S.J., Crouse, A.B., Hunter, J.M., Detloff, P.J. and Albin, R.L. (2005) Neuronal intranuclear inclusions and neuropil aggregates in HdhCAG(150) knockin mice. *Neuroscience*, **131**, 843–852.
30. Van Raamsdonk, J.M., Murphy, Z., Slow, E.J., Leavitt, B.R. and Hayden, M.R. (2005) Selective degeneration and nuclear localization of mutant huntingtin in the YAC128 mouse model of Huntington disease. *Hum. Mol. Genet.*, **14**, 3823–3835.
31. Wheeler, V.C., White, J.K., Gutekunst, C.A., Vrbanac, V., Weaver, M., Li, X.J., Li, S.H., Yi, H., Vonsattel, J.P., Gusella, J.F. *et al.* (2000) Long glutamine tracts cause nuclear localization of a novel form of huntingtin in medium spiny striatal neurons in HdhQ92 and HdhQ111 knock-in mice. *Hum. Mol. Genet.*, **9**, 503–513.
32. Davies, S.W., Turmaine, M., Cozens, B.A., DiFiglia, M., Sharp, A.H., Ross, C.A., Scherzinger, E., Wanker, E.E., Mangiarini, L. and Bates, G.P. (1997) Formation of neuronal intranuclear inclusions underlies the neurological dysfunction in mice transgenic for the HD mutation. *Cell*, **90**, 537–548.
33. Guttler, T., Madl, T., Neumann, P., Deichsel, D., Corsini, L., Monecke, T., Ficner, R., Sattler, M. and Gorlich, D. (2010) NES consensus redefined by structures of PKI-type and Rev-type nuclear export signals bound to CRM1. *Nat. Struct. Mol. Biol.*, **17**, 1367–1376.
34. Engelsma, D., Bernad, R., Calafat, J. and Fornerod, M. (2004) Supraphysiological nuclear export signals bind CRM1 independently of RanGTP and arrest at Nup358. *EMBO J.*, **23**, 3643–3652.
35. Guttler, T. and Gorlich, D. (2011) Ran-dependent nuclear export mediators: a structural perspective. *EMBO J.*, **30**, 3457–3474.
36. Kudo, N., Wolff, B., Sekimoto, T., Schreiner, E.P., Yoneda, Y., Yanagida, M., Horinouchi, S. and Yoshida, M. (1998) Leptomycin B inhibition of signal-mediated nuclear export by direct binding to CRM1. *Exp. Cell Res.*, **242**, 540–547.

37. Neville, M. and Rosbash, M. (1999) The NES-Crm1p export pathway is not a major mRNA export route in *Saccharomyces cerevisiae*. *EMBO J.*, **18**, 3746–3756.

38. Hilditch-Maguire, P., Trettel, F., Passani, L.A., Auerbach, A., Persichetti, F. and MacDonald, M.E. (2000) Huntingtin: an iron-regulated protein essential for normal nuclear and perinuclear organelles. *Hum. Mol. Genet.*, **9**, 2789–2797.

39. Tao, T. and Tartakoff, A.M. (2001) Nuclear relocation of normal huntingtin. *Traffic*, **2**, 385–394.

40. Yoshida, H., Matsui, T., Yamamoto, A., Okada, T. and Mori, K. (2001) XBP1 mRNA is induced by ATF6 and spliced by IRE1 in response to ER stress to produce a highly active transcription factor. *Cell*, **107**, 881–891.

41. Klebe, C., Bischoff, F.R., Ponstingl, H. and Wittinghofer, A. (1995) Interaction of the nuclear GTP-binding protein Ran with its regulatory proteins RCC1 and RanGAP1. *Biochemistry (Mosc)*. **34**, 639–647.

42. Keryer, G., Pineda, J.R., Liot, G., Kim, J., Dietrich, P., Benstaali, C., Smith, K., Cordelieres, F.P., Spassky, N., Ferrante, R.J. *et al.* (2011) Ciliogenesis is regulated by a huntingtin-HAP1-PCM1 pathway and is altered in Huntington disease. *J. Clin. Invest.*, **121**, 4372–4382.

43. Wang, W., Budhu, A., Forgues, M. and Wang, X.W. (2005) Temporal and spatial control of nucleophosmin by the Ran-Crm1 complex in centrosome duplication. *Nat. Cell Biol.*, **7**, 823–830.

44. Brodie, K.M., Mok, M.T. and Henderson, B.R. (2012) Characterization of BARD1 targeting and dynamics at the centrosome: the role of CRM1, BRCA1 and the Q564H mutation. *Cell. Signal.*, **24**, 451–459.

45. Dishinger, J.F., Kee, H.L., Jenkins, P.M., Fan, S., Hurd, T.W., Hammond, J.W., Truong, Y.N., Margolis, B., Martens, J.R. and Verhey, K.J. (2010) Ciliary entry of the kinesin-2 motor KIF17 is regulated by importin-beta2 and RanGTP. *Nat. Cell Biol.*, **12**, 703–710.

46. Fan, S., Fogg, V., Wang, Q., Chen, X.W., Liu, C.J. and Margolis, B. (2007) A novel Crumbs3 isoform regulates cell division and ciliogenesis via importin beta interactions. *J. Cell Biol.*, **178**, 387–398.

47. Fan, S., Whiteman, E.L., Hurd, T.W., McIntyre, J.C., Dishinger, J.F., Liu, C.J., Martens, J.R., Verhey, K.J., Sajjan, U. and Margolis, B. (2011) Induction of Ran GTP drives ciliogenesis. *Mol. Biol. Cell*, **22**, 4539–4548.

48. Hurd, T.W., Fan, S. and Margolis, B.L. (2011) Localization of retinitis pigmentosa 2 to cilia is regulated by Importin beta2. *J. Cell Sci.*, **124**, 718–726.

49. Kee, H.L., Dishinger, J.F., Lynne Blasius, T., Liu, C.J., Margolis, B. and Verhey, K.J. (2012) A size-exclusion permeability barrier and nucleoporins characterize a ciliary pore complex that regulates transport into cilia. *Nat. Cell Biol.*, **14**, 431–437.

50. Gray, M., Shirasaki, D.I., Cepeda, C., Andre, V.M., Wilburn, B., Lu, X.H., Tao, J., Yamazaki, I., Li, S.H., Sun, Y.E. *et al.* (2008) Full-length human mutant huntingtin with a stable polyglutamine repeat can elicit progressive and selective neuropathogenesis in BACHD mice. *J. Neurosci.*, **28**, 6182–6195.

51. Coyle, J.H., Bor, Y.C., Rekosh, D. and Hammarskjold, M.L. (2011) The Tpr protein regulates export of mRNAs with retained introns that traffic through the Nxf1 pathway. *RNA*, **17**, 1344–1356.

52. David-Watine, B. (2011) Silencing nuclear pore protein Tpr elicits a senescent-like phenotype in cancer cells. *PLoS One*, **6**, e22423.

53. Ben-Efraim, I., Frosst, P.D. and Gerace, L. (2009) Karyopherin binding interactions and nuclear import mechanism of nuclear pore complex protein Tpr. *BMC Cell Biol.*, **10**, 74.

54. Clarke, P.R. and Zhang, C. (2008) Spatial and temporal coordination of mitosis by Ran GTPase. *Nat. Rev. Mol. Cell Biol.*, **9**, 464–477.

55. Brodie, K.M. and Henderson, B.R. (2012) Characterization of BRCA1 protein targeting, dynamics, and function at the centrosome: a role for the nuclear export signal, CRM1, and Aurora A kinase. *J. Biol. Chem.*, **287**, 7701–7716.

56. Neuber, A., Franke, J., Wittstruck, A., Schlenstedt, G., Sommer, T. and Stade, K. (2008) Nuclear export receptor Xpo1/Crm1 is physically and functionally linked to the spindle pole body in budding yeast. *Mol. Cell Biol.*, **28**, 5348–5358.

57. Keryer, G., Di Fiore, B., Celati, C., Lechtreck, K.F., Mogensen, M., Delouvee, A., Lavia, P., Bornens, M. and Tassin, A.M. (2003) Part of Ran is associated with AKAP450 at the centrosome: involvement in microtubule-organizing activity. *Mol. Biol. Cell*, **14**, 4260–4271.

58. Han, X., Saito, H., Miki, Y. and Nakanishi, A. (2008) A CRM1-mediated nuclear export signal governs cytoplasmic localization of BRCA2 and is essential for centrosomal localization of BRCA2. *Oncogene*, **27**, 2969–2977.

59. Nakanishi, A., Han, X., Saito, H., Taguchi, K., Ohta, Y., Imajoh-Ohmi, S. and Miki, Y. (2007) Interference with BRCA2, which localizes to the centrosome during S and early M phase, leads to abnormal nuclear division. *Biochem. Biophys. Res. Commun.*, **355**, 34–40.

60. Godin, J.D., Colombo, K., Molina-Calavita, M., Keryer, G., Zala, D., Charrin, B.C., Dietrich, P., Volvert, M.L., Guillemot, F., Dragatsis, I. *et al.* (2010) Huntingtin is required for mitotic spindle orientation and mammalian neurogenesis. *Neuron*, **67**, 392–406.

61. Giannini, A., Mazor, M., Orme, M., Vivanco, M., Waxman, J. and Kypta, R. (2004) Nuclear export of alpha-catenin: overlap between nuclear export signal sequences and the beta-catenin binding site. *Exp. Cell Res.*, **295**, 150–160.

62. Desmond, C.R., Atwal, R.S., Xia, J. and Truant, R. (2012) Identification of a Karyopherin beta1/beta2 proline-tyrosine nuclear localization signal in huntingtin protein. *J. Biol. Chem.*, **287**, 39626–39633.

63. Obado, S.O. and Rout, M.P. (2012) Ciliary and nuclear transport: different places, similar routes? *Dev. Cell.* **22**, 693–694.

64. Truant, R. and Cullen, B.R. (1999) The arginine-rich domains present in human immunodeficiency virus type 1 Tat and Rev function as direct importin beta-dependent nuclear localization signals. *Mol. Cell Biol.*, **19**, 1210–1217.

65. Wang, L., Charroux, B., Kerridge, S. and Tsai, C.C. (2008) Atrophin recruits HDAC1/2 and G9a to modify histone H3K9 and to determine cell fates. *EMBO Rep.* **9**, 555–562.

66. Trettel, F., Rigamonti, D., Hilditch-Maguire, P., Wheeler, V.C., Sharp, A.H., Persichetti, F., Cattaneo, E. and MacDonald, M.E. (2000) Dominant phenotypes produced by the HD mutation in STHdh(Q111) striatal cells. *Hum. Mol. Genet.*, **9**, 2799–2809.

67. Carpenter, A.E., Jones, T.R., Lamprecht, M.R., Clarke, C., Kang, I.H., Friman, O., Guertin, D.A., Chang, J.H., Lindquist, R.A., Moffat, J. *et al.* (2006) CellProfiler: image analysis software for identifying and quantifying cell phenotypes. *Genome Biol.* **7**, R100.